

FTMP-based Simulation and Continuum Description of Discrete Dislocation System

*Motoki Uematsu¹ and Tadashi Hasebe²

Graduate School of Engineering, Kobe University, 1-1 Rokkodai, Nada, Kobe 657-8501, Japan.

²Department of Mechanical Engineering, Faculty of Engineering, Kobe University,
1-1 Rokkodai, Nada, Kobe 657-8501, Japan.

*Corresponding author: 138t310t@stu.kobe-u.ac.jp

Abstract

This study proposes a method for a continuum description of discrete dislocation systems based on Field Theory of Multiscale Plasticity (FTMP). Dislocations are linear defects generally extended in 3D space in complex manners: They can be bent (or curved), mutually tangle, multiply, annihilate and even yield topological changes (e.g., junction formations). Those pieces of information are discrete in nature and, at the same time, include complicated spatial details. FTMP-based incompatibility representation of the 3D dislocation system enables us to express not only the density-related information (i.e., change in the total length) but also those about the configurational changes such as rigid-body translations, local bowing-out and pinning-unpinning behaviors, including their directionalities, which are absent in the conventional dislocation density-based representation. The associated energy flow is also examined in detail based on the flow-evolutionary perspectives that relates the spatio-temporal fluctuation in the elastic strain energy with the incompatibility field.

Keywords: Field theory, Dislocation, Discrete dislocation dynamics, Incompatibility tensor, Continuum mechanics, crystalline plasticity

Introduction

Dislocation is a major carrier of plasticity in crystalline solids, which is often compared to “wrinkle” of a wide-spreading carpet as a tangible simile. Although dominant roles of dislocations have been well-recognized and well-documented to date, still there seem to be many mysteries remain unfolded, e.g., with respect to their critical roles in controlling micro/macroscale properties of the targeted crystalline materials. One of the reasons is that dislocations do not always determine the system response individually but frequently do as groups, like as substructures evolving during the course of elasto-plastic deformation. One of such eloquent examples is “dislocation cells” that are universally observed in plastically-deformed crystals [Kubin (1996), Raj and Phar (1986)], in the sense that they substantially controls the overall mechanical properties notwithstanding we do not essentially know why and how they are formed. Since the dislocation cells are composed of extremely large number of dislocations having roughly a periodic structure with wavelengths commensurate with submicron to micron, which is much larger than the magnitude of Burgers vector (characteristic (intrinsic) length of dislocation), it may safely be said that this dilemma is a critical “missing link” against achieving multiscale modeling of plasticity in terms of “transcending” scales.

To solve the above dilemma, we ought to establish, above all, how to view dislocation aggregates in coarse-grained manner, maintaining their linear nature including the configurational complexities when necessary. Figure 1 shows a schematic drawing for “discrete vs. continuum” dislocations in 2D and 3D. One can notice exclusive difficulties in expressing 3D discrete dislocations based on a continuum picture, whereas relatively easy method may be found for 2D counterparts such as using distribution functions like for aggregate of particles. We must admit almost nothing has been done in this respect since Kröner suggested a use of statistical mechanics in his approach based on multi-point dislocation correlation function for expressing distributed dislocations [Kröner (1970)].

This study extensively discusses a method for describing complex dislocation systems based on Field Theory of Multiscale Plasticity (FTMP) [Hasebe (2004), (2006), (2011)], taking an example of simplified dislocation arrangements, after briefly showing the FTMP-based 3D evaluation scheme. The example to be taken is about damping motions of dislocation segments, leading practically, e.g., to the apparent reduction in elastic moduli as a macroscopic mechanical response.

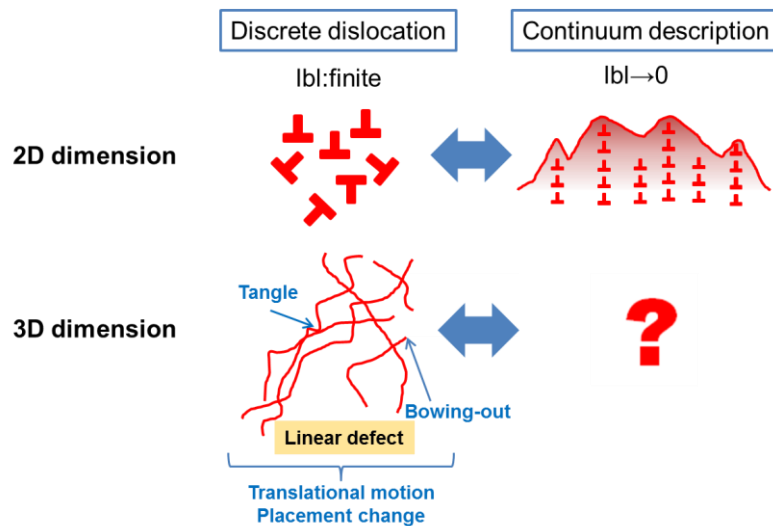


Figure 1. Discrete vs. continuum representations of dislocation aggregates.

About “Apparent” Reduction in Elastic Modulus

Experimentalists might have noticed decreasing elastic modulus observable in loading and reloading stress-strain curves [e.g., Yang, et al. (2004)], implying the elastic modulus (e.g., Young’s modulus) is not always be constant at least apparently during elasto-plastic deformation. This phenomenon causes many engineering problems, greatly affecting the predicting precisions of practically-important mechanical properties of metallic materials such as springback and the amount of ratcheting. Few studies, however, seem to have been carried out (this phenomenon seem to have not been taken so seriously by analytical researchers) probably and partially because of lack of such practical experiences.

The simplest mechanism yielding the “apparent” reduction in the elastic modulus is damping motions of pinned dislocation segments. During loading and unloading, pinned dislocation segments bow out and subsequently come back to the original configurations if there is no internal stress. This “reversible” plastic response consequently contributes to the “apparent softening” in the elastic stress-strain response, which appears as the apparent “reduction in the shear modulus.”

Let $\Delta\gamma_p$ be the recovered plastic strain and $\Delta\mu$ be the apparent decrement of the shear modulus caused by $\Delta\gamma_p$, we have,

$$\gamma^e + \Delta\gamma^p = [\mu^{-1} + \Delta\mu^{-1}] \tau = \mu^{-1} [1 + (\mu / \Delta\mu)] \tau \quad (1)$$

What we resultantly observe as the shear modulus from the given stress-strain response is $\mu [1 + (\mu / \Delta\mu)]^{-1}$ instead of μ . Therefore, the ‘‘apparent’’ reduction ratio of the shear modulus is given by,

$$\mu' / \mu \equiv [1 + (\mu / \Delta\mu)]^{-1} \quad (2)$$

where μ' denotes the shear modulus to be observed. Theoretically, μ' / μ can be evaluated as,

$$\mu' / \mu \equiv [1 + \ell^3 N / (6 \times L^3)]^{-1} \quad (3)$$

with N is the number of dislocation segments, while L and ℓ are the simulation cell size and the segment length, respectively.

Analytical Model and Procedure

FTMP-based Incompatibility Model and Duality Diagram Representation

Given 3D dislocation configurations, the dislocation density tensor α_{ij} is firstly evaluated for each sub-cell, where the simulation cell is divided into $10 \times 10 \times 10$ sub-cells in the present study. Here, a coarse-grained line vector is introduced for the dislocations contained in each sub-cell, without which all the details about the segment-wise geometrical fluctuations affect the distinction between edge and screw components. The definition of α_{ij} in this context is given as,

$$B_i = \alpha_{ji} dS_j \quad (4)$$

where B_i is the Burgers vector corresponding to the coarse-grained line vector and dS_j is the area through which the dislocations penetrate. Note the total length of the dislocations within the sub-cell is renormalized into the coarse-grained counterpart to conserve the density.

Based on the thus evaluated dislocation density tensor, the incompatibility tensor is further evaluated as,

$$\eta_{ij} = -(\epsilon_{ikl} \partial_k \alpha_{jl})_{SYM} \quad (5)$$

where the spatial derivative is evaluated for a given arbitrary coarse-grained region by utilizing the least-square method [Yoon (2011)].

According to the flow-evolutionary hypothesis [Hasebe (2013)] in FTMP, the incompatibility tensor is equated with the fluctuation part of the energy-momentum tensor, where both the tensors are defined in the four-dimensional space-time. The temporal components provides the following specific relationship (assuming static conditions),

$$\eta_{KK} = \kappa \delta U^e \quad (6)$$

where κ is named duality coefficient. Based on Eq.(6), we can draw duality diagrams, i.e., the relationship between the trace of the incompatibility tensor and (the fluctuation part of) the elastic strain energy. The duality diagram representation allows us to ‘‘visualize’’ the energy conversion process or ‘‘energy flow’’ in terms of dislocation movements within the system.

Analytical Conditions and Simulation Models

We perform a series of dislocation dynamics simulations [Zbib (2002)] for obtaining dislocation systems to be examined. Figure 2 shows the simulation cell with $(2000b)^3$ edges, together with a prescribed slip plane and Burgers vector. We assume α -Fe (BCC), with the density $7.88 \times 10^3 \text{ kg/m}^3$,

the shear modulus 80.0GPa, Poisson's ratio $\nu=0.324$, and the magnitude of Burgers vector $b=2.483\times 10^{-10}$ m. The external shear stress τ is applied as shown in Fig.2 until 500 steps (loading) and is then reversed until 1,000 steps (unloading), with the increment of the simulation time step being 1.8×10^{-12} sec.

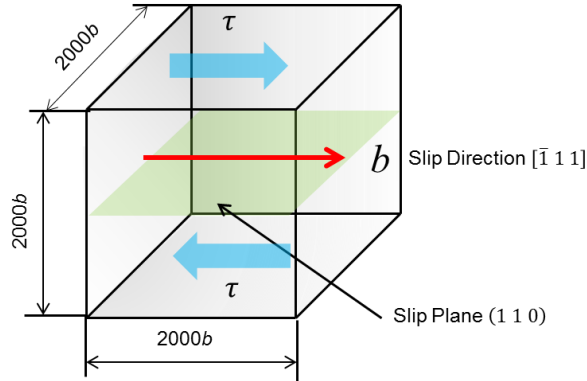


Figure 2. Schematic drawing of simulation cell.

Pinned dislocation segments are placed in the simulated cell as schematically shown in Fig.3, where the initial length of each segment is set to be $200b$ (b is the magnitude of Burgers vector). We consider roughly two arrangements of the dislocation segments, as shown in the figure, i.e. horizontal (Case A) and vertical (Case B) arrangements with respect to the slip plane. Note the Case B (vertical arrangement) may be regarded as a simplified model for dislocation walls.

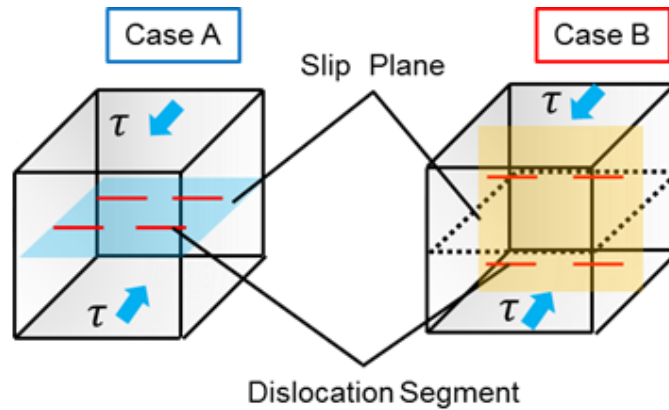


Figure 3. Schematics of simulation models with two representative dislocation arrangements, Case A (horizontal arrangement) and Case B (vertical arrangement).

Results and Discussions

Stress-strain response and apparent reduction in shear modulus

Figure 4 shows examples of simulation results for Case A and B with $N=175$, showing bowing-out dislocation segments. As observed in these snapshots, we immediately learn that the bowing-out motions are greatly restricted in Case B compared with Case A, probably due to the induced back stress field.

The corresponding shear stress-shear strain curves to the results in Fig.4 are presented in Fig.5. The restricted bowing-out motions of the dislocation segments for Case B results in much smaller slope of the diagram than those in Case A. Both the cases, however, exhibit nearly “reversible” stress-strain responses; the plastic shear strain caused by the bowing-out motions of dislocation segments is roughly recovered to zero when the bowed-out segments come back to the original configuration (i.e., straight line).

The corresponding “apparent” reduction ratios of the shear modulus to the results in Fig.5 are calculated by using Eq.(2) substituting $L = 2000b$ and $\ell = 200b$. Figure 6 shows variations of the “apparent” reduction rate of the shear modulus with increasing number of dislocation segments N , comparing Cases A, B and the theory given by Eq.(3). The results for Case A agree well with the theory, whereas Case B exhibits deviation from the theory as N increases. The deviation corresponds to the greatly-restricted bowing-out motions of dislocation segments seen in Fig.4.

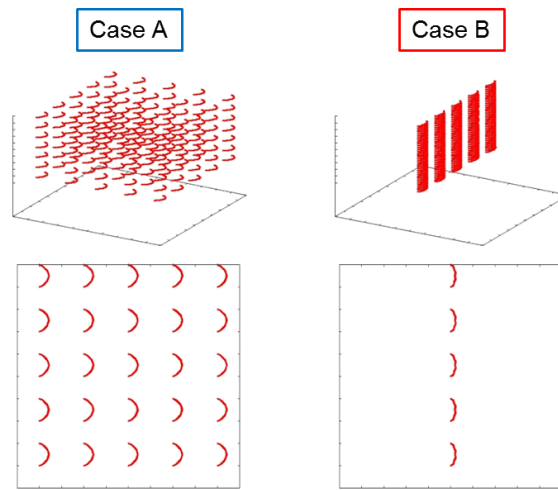


Figure 4. 3D and 2D snap shots of bowing-out dislocation segments for Case A and Case B (The number of dislocations is 175).

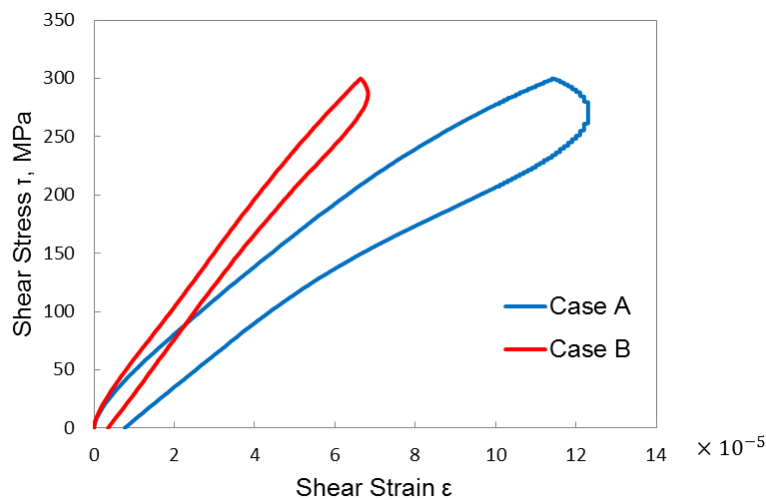


Figure 5. Shear stress-plastic shear strain responses for Cases A and B.

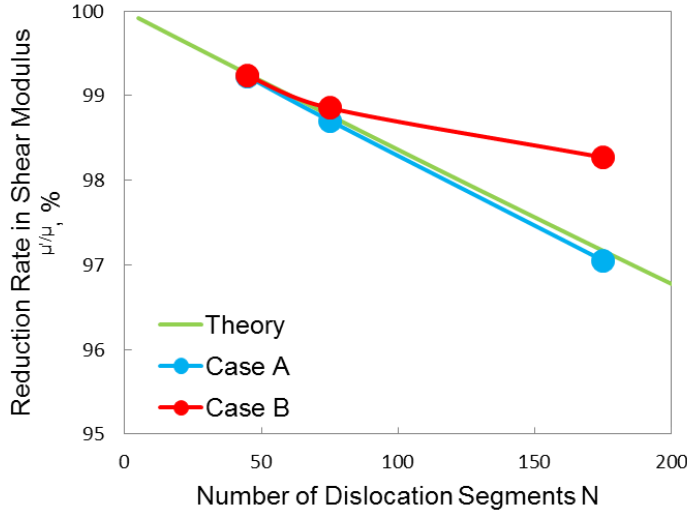


Figure 6. Relationship between “apparent” reduction rate in shear modulus and number of dislocation segments.

Duality diagram representation

We examine the above bowing-out responses of the dislocation segments based on the duality diagram representation based on the flow-evolutionary hypothesis [Hasebe (2013)]. Figure 7 displays a duality diagram for $N=175$, comparing between Cases A and B. One can observe a large difference between the two cases. As demonstrated, Case A exhibits a sharp increase in η almost vertically in the diagram, meaning most of the externally-applied work is consumed as the growth of the incompatibility, without being stored in the dislocations. In sharp contrast to this, in Case B, the incompatibility grows but the growth rate tends to saturate as the elastic strain energy increases. This indicates that the external energy is effectively stored in the bowing-out dislocation segments until the critical configuration is reached.

The above distinct trends between Case A and B well correspond to those in the bowing-out configurations of dislocation segments in Fig.4. Thus way, the energy flow associated with the configurational changes of the dislocations can be visualized via the duality diagram.

Let us discuss further the duality diagram in terms of the interrelationship with the system response, i.e., the apparent reduction in the shear modulus discussed above associated with Fig.6. it should be noted that the duality diagram displayed in Fig.7 does not take into account the contribution of the external work done by the applied stress in the abscissa, meaning the indicated energy flow is limited to the internal one solely associated with the configurational change of the dislocation segments, thus not directly representing the stress-strain response as a system. If we consider the contribution of the external work, the duality diagram can be redrawn as Fig.8, which is regarded as being reflected the response of the system. From this re-drawn diagram, we evaluate the duality coefficient via $\kappa \equiv \sum \eta / \sum U^e$, which measures how much strain energy is converted to (or dissipated into) local plasticity (the bowing-out motions of dislocation segments, in this case) that manifests itself as the growth of the incompatibility tensor.

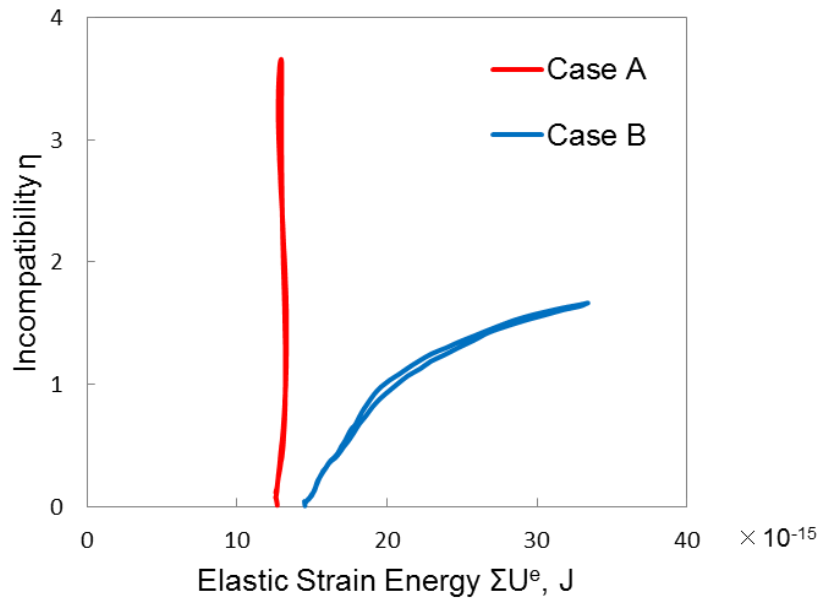


Figure 7. Duality diagram: relationship between η and ΣU^e (The number of dislocations is 175).

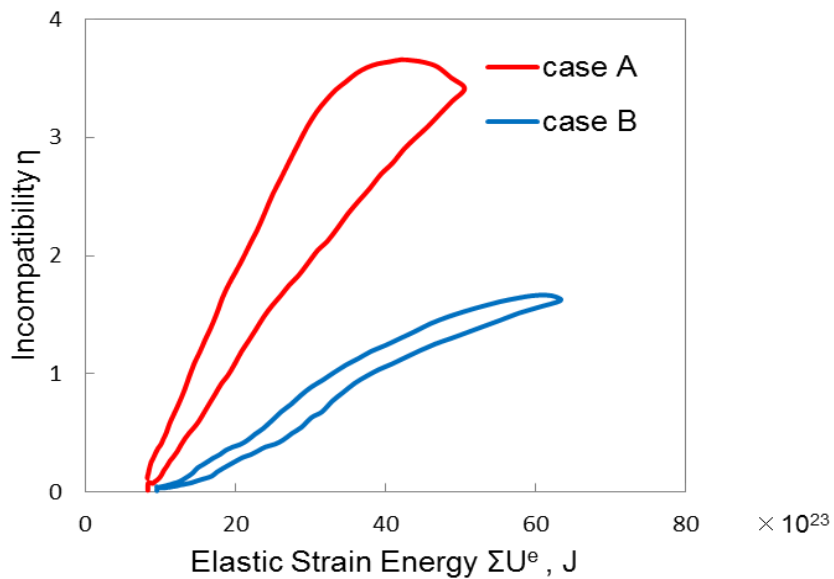


Figure 8. System-wise duality diagram: relationship between η and ΣU^e (The number of dislocations is 175).

Figure 9 correlates the apparent reduction rate of the shear modulus with the above-obtained duality coefficient. There observed a good correlation between the two regardless of the arrangements (Cases A and B) and the number of dislocation segments, implying the duality coefficient can be a parameter measuring the system response for the present dislocation systems.

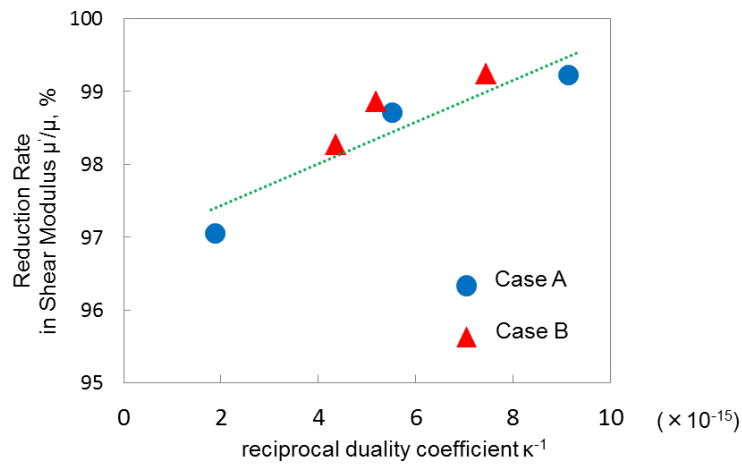


Figure 10. Relationship between reciprocal of duality coefficient and apparent reduction rate in shear modulus.

Conclusion

This study discusses FTMP-based continuum description of discrete dislocation systems, together with the duality diagram representation based on the flow-evolutionary hypothesis. Two typical dislocation arrangements yielding distinct bowing-out configurations of dislocation segments are examined in connection with the system response leading to the “apparent” reduction in the shear modulus. The configurational changes of the dislocation segments are demonstrated to be rationally expressed by the incompatibility tensor. The associated energy flow is shown to be successfully visualized by the duality diagram, while the duality coefficient provides a quantitative measures of the system response, i.e., apparent reduction rate of the shear modulus.

References

- Hasebe, T., (2004), “Field Theoretical Multiscale Modeling of Polycrystal Plasticity,” *Trans. MRS-J*, Vol.29, pp.3619-3624.
- Hasebe, T., (2006), “Multiscale Crystal Plasticity Modeling based on Field Theory,” *Comp. Mech. Eng. Sci. (CMES)*, **11-3**, 145-155.
- Hasebe, T., (2013), “Flow-Evolutionary Hypothesis based on Field Theory of Multiscale Plasticity (FTMP) and Its Applications,” Proc. APCOM2013.
- Kröner, E., (1970), “Initial Studies of a Plastic Theory based upon Statistical Mechanics,” in “Inelastic Behavior of Solids,” (Eds. Kanninen, M. F., et al.), p.137, McGraw-Hill.
- Kubin, L. P., “Dislocation Patterns: Experiment, Theory and Simulation,” in “Stability of Materials” (eds: Gonis, A., Turchi, P. E. A. and Kurdrnovsky, J.), *Procs. NATO Advanced Study Institute on Stability of Materials, 1994, Greece*, (1996), 99-133, Plenum Press.
- Raj, S. V. and Pharr, G. M., (1986), “Compilation and Analysis of Data for the Stress Dependence of the Subgrain Size, Mater. Sci. Eng., **81**, 217-237.
- Yang, M., et al. (2004) , “Materials Processing Technology” 151,232-236
- Yoon, I., (2012), “FTMP based Development of Continuous Field Evaluation Method for Three-Dimensional Discrete Dislocation System,” Undergraduate Thesis, Kobe University.
- Zbib, H. M. (2002), “Multiscale Dislocation Dynamics Plasticity For FCC and BCC Single Crystals Version 02”.